

## Hard-photon emission in $^{129}\text{Xe} + ^{197}\text{Au}$ reaction at 44 MeV/nucleon

Giuseppe Russo

*Dipartimento di Fisica, Università di Catania, Corso Italia, 57 - 95129 Catania, Italy  
and Istituto Nazionale di Fisica Nucleare, Laboratorio Nazionale del Sud, Catania, Italy*

(Received 15 July 1993)

Semi-exclusive measurements of high energy photons ( $E_\gamma \geq 30$  MeV) cross sections from the  $^{129}\text{Xe} + ^{197}\text{Au}$  reaction at 44 MeV/nucleon are analyzed in the framework of the Boltzmann-Nordheim-Vlasov equation with an appropriate semiclassical  $\gamma$ -production probability for the  $np \rightarrow n'p'\gamma$  elementary process. A detailed analysis on the impact parameter dependence of the  $\gamma$ -ray multiplicity and slope of the energy spectrum is also reported.

PACS number(s): 25.70.-z, 21.30.+y

### I. INTRODUCTION

Hard-photon production in intermediate energy heavy-ion reactions seems to be one of the experimental observables which is sensitive to the properties of nuclear matter at various densities and temperatures while it is not seriously affected by the final-state interactions [1]. Assuming  $\gamma$  emission from a single moving source, the analysis of the two-dimensional plot of the measured invariant photon cross sections versus rapidity and transverse energy provides source velocities which are, also for mass-asymmetric target-projectile combinations, in agreement with those expected if the origin of the radiation is mainly attributed to incoherent proton-neutron bremsstrahlung [2]. The comparison between the high energy photon production cross sections in nucleus-nucleus collisions (normalized by appropriate scaling factors which account for the projectile and target masses dependences) and in free  $p$ - $n$  collisions also evidences the important role played from the coupling of the nucleons' Fermi motion inside the projectile or target with the relative motion of the colliding nuclei. This accounts for the general trend of the hard-photon emission probability per in-medium neutron-proton collision as a function of the Coulomb corrected beam energy per nucleon.

The  $\gamma$ -ray energy spectra display, in the source frame and for energies larger than 30 MeV, an almost exponential behavior with a characteristic inverse slope parameter  $E_0$ . Such an inverse slope, which should be related to the hardness of the produced  $\gamma$  rays, has been measured in inclusive experiments over a wide range of projectile-target and bombarding energy combinations [2]. However, up to now, only in a few exclusive experiments has the inverse slope parameter been measured in coincidence with fragments [3] or light charged particles [4] or both [5] in order to investigate its impact parameter dependence. A heavier system, namely  $^{129}\text{Xe} + ^{197}\text{Au}$  at 44 MeV/nucleon, has been recently investigated by two different groups [6,7]. In these experiments, hard photons in coincidence with projectilelike fragments [6] and with light charged particles [7] in multidetector arrays having large solid angles were detected. The aim of this paper is the comparison of such semiexclusive experimental data

with theoretical predictions obtained from kinetic calculations using an appropriate semiclassical elementary  $\gamma$  production probability.

### II. THEORETICAL FRAMEWORK

For several years the nuclear dynamics in the intermediate energy domain has been treated within classical transport theories in which some quantum features such as Fermi motion and Pauli blocking are taken into account. One of the more successful semiclassical approaches is that based on the Boltzmann-Nordheim-Vlasov (BNV) equation. In this approach the nuclear many-body system is described by means of a time evolution equation for the one-body phase-space distribution function  $f(\mathbf{r}, \mathbf{p}, t)$  in a dynamics ruled by the competition of mean field and two-body collisions effects, namely

$$\frac{\partial f}{\partial t} + \{f, h\} = I_{\text{coll}}(f), \quad (1)$$

where  $\{ \}$  represent the Poisson brackets and  $I_{\text{coll}}$  is the collision integral, assumed of Uehling-Uhlenbeck type. The study of heavy-ion collisions by means of Eq. (1) is essentially a numerical task which is generally solved using the pseudoparticles method [8]. In the actual numerical simulation, the BNV equation is separated into classical Hamiltonian equations of motion for the propagation of the pseudoparticles, which are governed by an appropriate mean field and the stochastic two-body collisions during this propagation caused by the residual nucleon-nucleon ( $NN$ ) interaction. Therefore, there are two essential ingredients, the mean field potential and the in-medium  $NN$  scattering cross section. In the calculation of particle production rates, such as  $\gamma$ ,  $\pi$ ,  $K$ , etc., additional cross sections for the elementary processes are also needed. For our purpose, since the contribution of the  $pn\gamma$  process to the total  $NN$  cross section is about of the order  $10^{-4}$ , we may treat perturbatively the photon production and neglect the recoil momentum for the final nucleons in the calculation of the time evolution of the heavy-ion (HI) system. For more details on the numeri-

cal solution technique of the BNV equation we direct the reader to previous papers [8–10] and references therein. Here, only a very brief account on the hard gamma production will be given. Assuming photons are produced in individual  $pn$  collisions, which are sufficiently separated in space-time, the invariant double-differential photon production probability in a HI collision, at a fixed impact parameter  $b$ , is given by summing incoherently contributions from  $pn$  collisions at all time steps via

$$\frac{1}{E_\gamma} \frac{d^2 P_\gamma(b)}{dE_\gamma d\Omega_\gamma} = \sum_{np \text{ coll}} \int \frac{d\Omega_q}{4\pi} \frac{1}{E'_\gamma} \frac{d^2 P_{np\gamma}^{\text{elem}}}{dE'_\gamma d\Omega'_\gamma} P(\mathbf{r}, \mathbf{p}_3, \mathbf{p}_4, t), \quad (2)$$

where  $\mathbf{r}$  and  $t$  indicate the space-time coordinates. The prime denotes quantities in the individual neutron-proton center-of-mass system, which have to be Lorentz transformed to the laboratory frame. From energy-momentum conservation, the final nucleon momenta  $\mathbf{p}_3$  and  $\mathbf{p}_4$  are fixed by specifying the initial momenta  $\mathbf{p}_1$  and  $\mathbf{p}_2$ , the photon momentum  $\mathbf{p}_\gamma$ , and the direction  $\hat{\Omega}_q$  of the relative momentum  $\mathbf{q} = \mathbf{p}_3 - \mathbf{p}_4$  between the final nucleons:  $P(\mathbf{r}, \mathbf{p}_3, \mathbf{p}_4, t) = [1 - \bar{f}(\mathbf{r}, \mathbf{p}_3, t)][1 - \bar{f}(\mathbf{r}, \mathbf{p}_4, t)]$  is the final-state Pauli blocking factor determined from

$$\frac{d^2 P_{np\gamma}^{\text{elem}}}{dE_\gamma d\Omega_\gamma} = \frac{1}{E_\gamma} \frac{\alpha}{(2\pi)^2} [\beta_i^2 \sin^2 \Theta_i + \frac{2}{3} \beta_f^2] \left[ 1 + \frac{1}{2} \frac{m}{m_\pi} \left( \frac{m}{m_\pi} - 1 \right) \frac{\left( \frac{E_\gamma}{m_\pi c^2} \right)^2}{4 + \left( \frac{E_\gamma}{m_\pi c^2} \right)^2} \right] \quad (3)$$

with

$$\beta_f = \left[ \beta_i^2 - \frac{E_\gamma}{mc^2} - \left( \frac{E_\gamma}{2mc^2} \right)^2 \right]^{\frac{1}{2}} \hat{\mathbf{q}} - \frac{E_\gamma}{2mc^2} \hat{\mathbf{p}}_\gamma. \quad (4)$$

Here,  $\beta_{i,f} = \mathbf{p}_{i,f}/mc$  are the velocities (in  $c$  units) of the proton before and after the collision,  $\alpha$  is the fine-structure constant,  $\Theta_i$  is the polar angle formed from  $\beta_i$  and the direction of sight, and  $m_\pi c^2 \simeq 138$  MeV is the rest energy of the exchanged pion. The last factor in Eq. (3) (in the following called exchange factor) with respect to the expression of Ref. [11] accounts for the bremsstrahlung from virtual pions. In Fig. 1 we show a comparison between calculated double-differential cross sections at  $90^\circ$  for  $np$  bremsstrahlung at 170 MeV neutron laboratory energy, averaged over the nucleons' final relative angle  $\hat{\Omega}_q$ , with and without the exchange factor and the first measured  $\gamma$  spectrum from Malek *et al.* [14]. Since experimentally the neutron energy profile had a FWHM of about 70 MeV, we have folded the theoretical cross sections with a Gaussian in energy having the same width. The full and dashed lines are the classical soft-photon limit with and without the exchange factor, respectively. As it was also found in quantal calculations [12], the most noticeable feature of our semiclassical approach [Eq. (3)] with respect to the classical one is the increase of the photon production for energies larger than about 30 MeV. This rise is due to the presence of

the occupation probabilities of the final nucleons in the phase space [8].

The most important ingredient in these calculations is the elementary  $np \rightarrow n'p'\gamma$  probability. The simplest expression is Jackson's classical long-wavelength approximation [11], which does not include radiation from exchanged charged pions. Some attempts of quantum mechanical calculations, including convection, magnetic, and meson exchange current contributions have been successfully proposed [12]. One of the most interesting results of a quantal approach is the large effect of the so-called "internal radiation" (i.e., bremsstrahlung from the exchanged charged mesons) which interferes constructively with the external radiation (i.e., classical bremsstrahlung from the external lines of the Feynman graph). However, for practical applications in BNV calculations it is useful to have an analytical representation of the double-differential elementary  $\gamma$  cross section which is generally not available from quantal approaches. For this reason, as proposed in Ref. [13], we use a modified classical formula which contains approximatively the contribution of charged pion exchange. In the initial  $p$ - $n$  c.m. frame, after averaging over the direction of the final nucleon and in the soft-photon limit, it reads

the charged-meson exchange, which allows the proton to be scattered backwards with a corresponding large acceleration and radiation. Thus, we find our results in fair agreement with the first direct measurement of the  $\gamma$  spectrum in the free  $np$  collision.

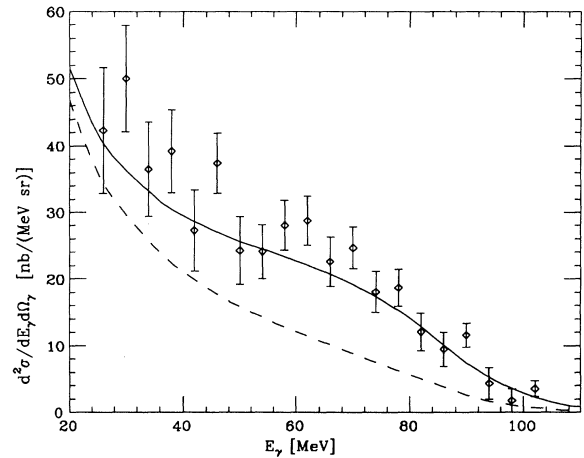


FIG. 1. Comparison between the photon spectrum measured at  $90^\circ$  in the  $np$  scattering at 170 MeV of neutron energy [14] (points) with theoretical calculations, in the soft-photon limit, with (full line) and without (dashed line) internal radiation from virtual pions.

### III. COMPARISON WITH EXPERIMENTAL DATA

First we would like to look at the inclusive data. In Table I, measured slopes of the energy spectra and total cross sections for the hard- $\gamma$  production from the  $^{129}\text{Xe} + ^{197}\text{Au}$  reaction at 44 MeV/nucleon [6,7] are compared with theoretical predictions. The inverse slope parameters, reported in round brackets, are our values obtained after correction for the BaF<sub>2</sub> detector response function. It was made by recalling that the measured spectrum  $Y(E)$  is related to the emitted one  $N(E)$  through the expression

$$Y(E') = \int_{E'}^{+\infty} N(E)K(E, E')dE, \quad (5)$$

where the kernel  $K(E, E')$  represents the detector response function. By assuming as an analytical expression,

$$K(E, E') = A(E) \exp\left[-\frac{(E' - E)^2}{\sigma^2}\right] \Theta(E' - E) \quad (6)$$

with  $\Theta(x)$  the step function [namely  $\Theta(x)=1$  if  $x < 0$  and  $\Theta(x) = 0$  otherwise],  $A(E)$  determined from the  $\int_0^E K(E, E')dE'=1$  condition and  $N(E) \propto \exp(-E/E_0)$ , we approximatively find

$$Y(E') \propto \exp\left(-\frac{E'}{E_0}\right) \exp\left[\frac{\alpha^2}{4E_0^2}E'^2\right] \text{erfc}\left[\frac{\alpha E'}{2E_0}\right]. \quad (7)$$

It provides an unfolded inverse slope parameter which, to the first order in the ratio  $\alpha = \sigma/E = (1/\ln 2)\Delta E'/E$ , is given by

$$E_0 \geq -\left[\frac{d \ln Y(E')}{dE'}\right]^{-1} \left(1 + \frac{\alpha}{\sqrt{\pi}}\right). \quad (8)$$

For our calculation we have assumed an energy resolution

TABLE I. Values of the inverse slope parameter, total photon cross section, probability of emitting photon per proton-neutron collision, and average number of first chance  $n$ - $p$  collisions for the  $^{129}\text{Xe} + ^{197}\text{Au}$  reaction at 44 MeV/nucleon. The (a) and (b) values refer to our BNV calculations with and without contribution from internal radiation. Values in parentheses in the first column, are obtained from the corresponding experimental data by correcting for the detector response function as described in the text. The value in parentheses in the last column should represent the theoretical prediction without Pauli blocking effect.

Apparatus or method	$E_0$ (MeV)	$\sigma_\gamma$ (mb)	$10^5 \langle P_{np\gamma} \rangle$	$\langle N_{np} \rangle_b$
TAPS [6]	12.0±0.1	4.9±0.9	5.2±0.8	15.2
( $E_\gamma \geq 30$ MeV)	(13.2±0.11)			
MEDEA [7]	13.6±0.4	3.8±0.4	4.7±0.5	17.3
( $E_\gamma \geq 40$ MeV)	(14.96±0.44)			
(a) Our BNV	18.6±0.9	3.3±0.2	4.3±0.2	11.05
( $E_\gamma \geq 40$ MeV)				(24.01)
(b)	15.6±0.6	1.4±0.1	1.8±0.1	

of  $\Delta E'/E = 0.12$ , in reasonable agreement with both the experimental and simulated data [15]. We note that the BNV calculation taking into account the radiation from virtual charged pion exchange, although providing a reasonable value of the overall  $\gamma$  yield, overestimates the inverse slope parameter by a factor 1.2.

Concerning the exclusive data, two observables have been used to measure the impact parameter: (1) the multiplicity of light charged particles (LCP) [7] and (2) the mass of the projectilelike fragments (PLF) [6]. They are sensitive in two different regions of the impact parameter scale; the first for central, medium, and quasiperipheral collisions and the latter for very peripheral collisions only. On the contrary, the PLF method is able to select very small steps in the impact parameter whereas the method using LCP multiplicity, because of statistical fluctuations on the particle emission, is less accurate. Experimentally, the in-medium average photon production probability  $\langle P_{np\gamma} \rangle$  for the elementary process is obtained by using a simple factorization of the  $\gamma$ -ray multiplicity in nucleus-nucleus collisions, namely

$$M_\gamma(b) \equiv \frac{d\sigma_\gamma/db}{d(\pi b^2)/db} \simeq \langle P_{np\gamma} \rangle N_{np}(b), \quad (9)$$

where  $N_{np}(b)$  is the number of first chance  $n$ - $p$  collisions at a given impact parameter  $b$ . An estimate of such a number is generally made within the equal-participant geometrical model [16] where it is assumed to be proportional to the volume of the overlap region for that  $b$ . We would like to stress that Eq. (2), when integrated both over energy and angle of the photon, approximatively provides, as a function of the impact parameter, a  $\gamma$ -ray multiplicity given by

$$M_\gamma(b) \simeq \langle P_{np\gamma} \rangle [N_{np}(b)P]. \quad (10)$$

Thus, our factorization also contains the Pauli blocking factor whose actions strongly reduce the effective average number of available  $n$ - $p$  collisions, represented in square brackets in Eq. (10).

In Fig. 2 we display, as a function of the impact parameter, the number of first chance  $n$ - $p$  collisions for the  $^{129}\text{Xe} + ^{197}\text{Au}$  reaction at 44 MeV/nucleon, as obtained from the geometrical method [16] compared with the results of BNV calculations with and without the Pauli blocking factor. We note the strong effect of the Pauli blocking factor, making unjustified the usual factorization [Eq. (9)] for the  $\gamma$ -ray production cross section in the nucleus-nucleus collision, introduced in order to obtain quantities for the elementary process as well as scaling laws. Central collisions are partially forbidden due to the action of the Pauli blocking factor while the peripheral ones are enhanced probably due to collisions outside the geometrical overlap zone all ignored in the equal-participant model.

In the last two columns of Table I, the in-medium total  $\gamma$ -ray production probability for the  $np\gamma$  elementary process and the number of first chance  $np$  collisions averaged over the impact parameter  $\langle N_{np} \rangle_b$  are also reported. Although within the experimental uncertainties

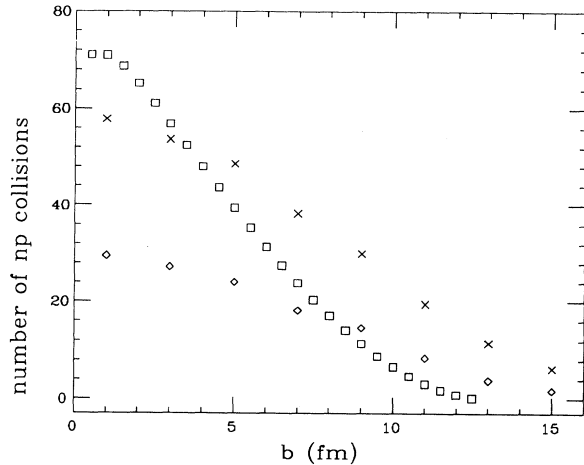


FIG. 2. Number of first chance  $n$ - $p$  collisions for the  $^{129}\text{Xe} + ^{197}\text{Au}$  reaction at 44 MeV/nucleon versus the impact parameter. Squares: geometrical model of Ref. [16]; diamonds and crosses represent microscopic BNV calculations with and without Pauli blocking factor.

we observe a general agreement between experimental and theoretical photon production probabilities, a significant difference in the average  $n$ - $p$  number of collisions is found. The BNV calculations provide a  $\langle N_{np} \rangle_b$  value which is reduced from 24.01 to 11.05 when it is corrected for the Pauli blocking factor while the value provided from the geometrical model [16] is in between these two values. Because of the observed discrepancies between experimental  $\gamma$  data currently available we do not expect appreciable changes in the systematics [17] of the photon emission probabilities based on the factorization of the inclusive photon multiplicity as obtained by integrating Eq. 9 over the impact parameter. On the contrary, significant effects emerge from the analysis of the exclusive photon cross section than we are showing.

In Fig. 3(a) our BNV calculation of the hard-photon multiplicity ( $E_\gamma \geq 40$  MeV) as a function of the impact parameter, obtained by Eqs. (2) and (3), is compared with both the experimental data of Refs. [6,7]. The error bars in the BNV data take into account the finite number of Gaussians per nucleon. A strong decrease of the  $\gamma$ -ray yield with increasing impact parameter, confirming the centrality of the hard-photon production, is found. In Fig. 3(b) the average probability of bremsstrahlung radiation in an individual  $n$ - $p$  collision, resulting from Eq. 10, is also reported. Its impact parameter independence is consistent with the incoherent  $n$ - $p$  bremsstrahlung assumption and consequently indicates the effective number of first chance  $n$ - $p$  collisions as the main responsibility on the strong impact parameter dependence of the hard-photon multiplicity.

In Fig. 4 we compare, as functions of the impact parameter, the experimental value of the inverse slope parameter extracted from the unfolded hard-photon spectrum [6,7] with the corresponding theoretical BNV calculation. Calculations including the internal radiation process (diamonds) still overestimate the data by a factor 1.2 on average while incidentally those obtained using

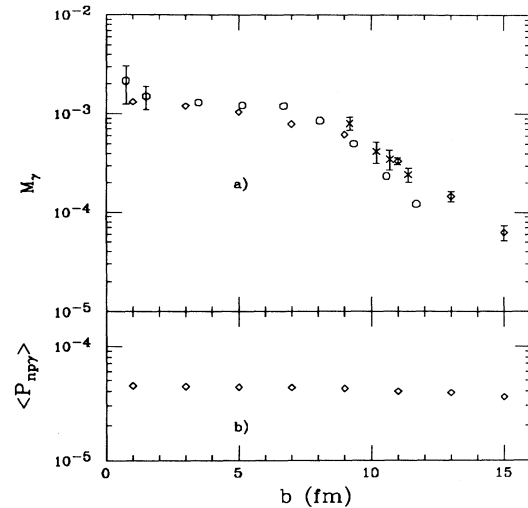


FIG. 3. Hard-photon multiplicity for nucleus-nucleus  $M_\gamma$  and for in-medium single proton-neutron  $\langle P_{np\gamma} \rangle$  collisions from the  $^{129}\text{Xe} + ^{197}\text{Au}$  reaction at 44 MeV/nucleon versus the impact parameter. Diamond points are our BNV calculations including internal radiation contribution ( $E_\gamma \geq 40$  MeV); circles and crosses are experimental values from Refs. [7,6] for photon energies greater than 40 and 30 MeV, respectively.

the classical Jackson expression [11] for the elementary process (squares) seem to agree very well with the experimental data. Anyway, both calculations predict a slow decrease of  $E_0$  with increasing  $b$  up to about the 9-fm value followed by a steeper decrease for a larger impact parameter in agreement with the data of Refs. [7,6], respectively. Thus, the general trend of  $E_0$  versus  $b$  seems to be confirmed, with the initial quasiflat behavior depending on the size of the colliding nuclei.

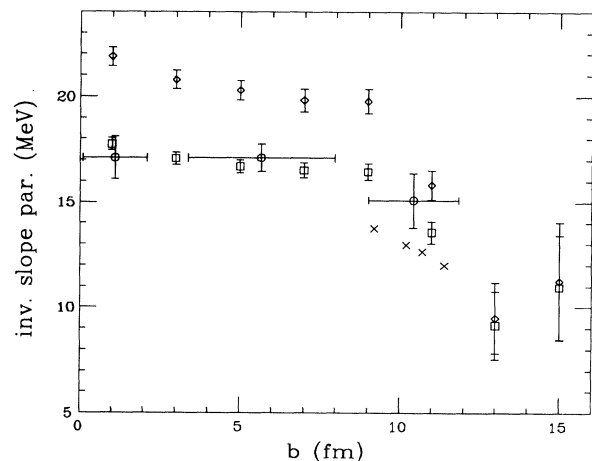


FIG. 4. Inverse slope parameter of the photon spectra from the  $^{129}\text{Xe} + ^{197}\text{Au}$  reaction at 44 MeV/nucleon as a function of the impact parameter. The same symbols as in Fig. 3 are used. The cross points are the experimental values of Ref. [6] after our unfolding procedure by means of Eq. (8). Square points are present BNV calculations without internal radiation contribution.

#### IV. CONCLUSIONS

In summary, we have made a detailed study on the dependence of the high-energy photon production from the impact parameter for the  $^{129}\text{Xe} + ^{197}\text{Au}$  reaction at 44 MeV/nucleon. We observed that both  $E_0$  and  $M_\gamma$  increase with increasing centrality of the collisional event. This result is consistent with the data of Refs. [3,4] and with previous calculations [8,10] on lighter systems. Calculations based on the BNV equation for the time development of the one-body phase-space distribution function and photon production via incoherent neutron-proton collisions reproduce very well the in-medium overall photon multiplicity but slightly overestimate the in-

verse slope parameter of the energy spectrum. It should be noticed that the geometrical model [16], based on the equal-participant hypothesis, does not correctly account for the impact parameter dependence of the number of first chance  $n$ - $p$  collisions. In fact, the dynamical BNV approach indicates that central collisions are strongly reduced due to the action of the Pauli blocking factor while the peripheral ones are enhanced with respect to the prediction of the geometrical model due to  $n$ - $p$  collisions which take place outside the overlap volume of the colliding nuclei. Moreover, the in-medium  $\gamma$ -ray multiplicity versus the impact parameter reflects, on average, the trend of the effective number of first chance  $n$ - $p$  collisions as predicted from the dynamical BNV approach.

- 
- [1] G.F. Bertsch and S. Das Gupta, *Phys. Rep.* **160**, 189 (1988); H. Stocker and W. Greiner, *ibid.* **137**, 277 (1986); W. Cassing, V. Metag, U. Mosel, and K. Niita, *ibid.* **188**, 363 (1990).
- [2] H. Nifenecker and J.A. Pinston, *Prog. Part. Nucl. Phys.* **23**, 271 (1989), and references therein.
- [3] R. Hingmann *et al.*, *Phys. Rev. Lett.* **58**, 759 (1987); S. Riess *et al.*, *ibid.* **69**, 1504 (1992); N. Herrmann *et al.*, *ibid.* **60**, 1630 (1988).
- [4] M. Kwato Njock *et al.*, *Nucl. Phys.* **A489**, 368 (1988); M. Kwato Njock *et al.*, *ibid.* **A488**, 503c (1988); H. Nifenecker, M. Kwato Njock, and J.A. Pinston, *ibid.* **495**, 3c (1989); T. Reposeur *et al.*, *Phys. Lett. B* **276**, 418 (1992).
- [5] L.G. Sobotka *et al.*, *Phys. Rev. C* **44**, 2257 (1991).
- [6] R. Merrouch *et al.*, *Nouv. Ganil* **38**, 4 (1991); G. Martínez *et al.*, *ibid.* **44**, 43 (1993); R.S. Mayer *et al.*, *Phys. Rev. Lett.* **70**, 904 (1993).
- [7] E. Migneco *et al.*, *Phys. Lett. B* **298**, 46 (1993).
- [8] G.F. Bertsch, H. Kruse, and S. Das Gupta, *Phys. Rev. C* **29**, 675 (1984); H. Kruse, B. Jacak, and H. Stocker, *Phys. Rev. Lett.* **54**, 289 (1985); J. Aichelin and G.F. Bertsch, *Phys. Rev. C* **31**, 1730 (1985); W. Bauer, G.F. Bertsch, W. Cassing, and U. Mosel, *ibid.* **34**, 2127 (1986).
- [9] A. Bonasera, G.F. Burgio, and M. Di Toro, *Phys. Lett. B* **221**, 233 (1989); A. Bonasera, G.F. Burgio, F. Gulminelli, and H.H. Wolter, *Nuovo Cimento A* **103**, 309 (1990); A. Bonasera, G. Russo, and H.H. Wolter, *Phys. Lett. B* **246**, 337 (1990); A. Bonasera and G. Russo, *Nuovo Cimento A* **105**, 301 (1992).
- [10] G. Russo, *J. Phys. G* **18**, 943 (1992).
- [11] J.D. Jackson, *Classical Electrodynamics* (Wiley, New York, 1962).
- [12] K. Nakayama, *Phys. Rev. C* **39**, 1475 (1989); K. Nakayama and G.F. Bertsch, *ibid.* **40**, 685 (1989); V. Hermann, J. Speth, and K. Nakayama, *ibid.* **43**, 394 (1991); M. Schafer, T.S. Biro, W. Cassing, U. Mosel, H. Nifenecker, and J.A. Pinston, *Z. Phys.* **339**, 391 (1991); D. Neuhaser and S.E. Koonin, *Nucl. Phys.* **A462**, 163 (1987).
- [13] G. Russo, *Nucl. Phys. A* (to be published).
- [14] F. Malek, H. Nifenecker, J.A. Pinston, F. Schussler, S. Drissi, and J. Julien, *Phys. Lett. B* **266**, 255 (1991).
- [15] R. Novotny *et al.*, *Nucl. Instrum. Methods A* **262**, 340 (1987); A. Badalá *et al.*, *ibid.* **306**, 283 (1991).
- [16] H. Nifenecker and J.P. Bondorf, *Nucl. Phys.* **A442**, 478 (1985).
- [17] V. Metag, *Nucl. Phys.* **A488**, 483c (1988); **553**, 283c (1993); *Prog. Part. Nucl. Phys.* **30**, 75 (1993).